

Intraoperative Assessment of Tumor Resection Margins in Breast-Conserving Surgery Using ^{18}F -FDG Cerenkov Luminescence Imaging: A First-in-Human Feasibility Study

Maarten R. Grootendorst^{1,2}, Massimiliano Cariati^{1,2}, Sarah E. Pinder¹, Ashutosh Kothari², Michael Douek^{1,2}, Tibor Kovacs², Hisham Hamed², Amit Pawa³, Fiona Nimmo⁴, Julie Owen¹, Vernie Ramalingam², Sweta Sethi², Sanjay Mistry², Kunal Vyas⁵, David S. Tuch⁶, Alan Britten⁷, Mieke Van Hemelrijck¹, Gary J. Cook⁸, Chris Sibley-Allen⁹, Sarah Allen⁹, and Arnie Purushotham^{1,2}

¹Division of Cancer Studies, King's College London, London, United Kingdom; ²Department of Breast Surgery, Guy's and St Thomas' NHS Foundation Trust, London, United Kingdom; ³Anesthetic Department, Guy's and St Thomas' NHS Foundation Trust, London, United Kingdom; ⁴Day Surgery Unit, Guy's and St Thomas' NHS Foundation Trust, London, United Kingdom; ⁵Sagentia Ltd., Cambridge, United Kingdom; ⁶Lightpoint Medical Ltd., Chesham, United Kingdom; ⁷Medical Physics Department, St George's Hospital, London, United Kingdom; ⁸Division of Imaging Sciences and Biomedical Engineering, King's College London, London, United Kingdom; and ⁹Department of Nuclear Medicine, Guy's and St Thomas' NHS Foundation Trust, London, United Kingdom

In early-stage breast cancer, the primary treatment option for most women is breast-conserving surgery (BCS). There is a clear need for more accurate techniques to assess resection margins intraoperatively, because on average 20% of patients require further surgery to achieve clear margins. Cerenkov luminescence imaging (CLI) combines optical and molecular imaging by detecting light emitted by ^{18}F -FDG. Its high-resolution and small size imaging equipment make CLI a promising technology for intraoperative margin assessment. A first-in-human study was conducted to evaluate the feasibility of ^{18}F -FDG CLI for intraoperative assessment of tumor margins in BCS. **Methods:** Twenty-two patients with invasive breast cancer received ^{18}F -FDG (5 MBq/kg) 45–60 min before surgery. Sentinel lymph node biopsy was performed using an increased $^{99\text{m}}\text{Tc}$ -nanocolloid activity of 150 MBq to facilitate nodal detection against the γ -probe background signal (cross-talk) from ^{18}F -FDG. The cross-talk and $^{99\text{m}}\text{Tc}$ dose required was evaluated in 2 lead-in studies. Immediately after excision, specimens were imaged intraoperatively in an investigational CLI system. The first 10 patients were used to optimize the imaging protocol; the remaining 12 patients were included in the analysis dataset. Cerenkov luminescence images from incised BCS specimens were analyzed postoperatively by 2 surgeons blinded to the histopathology results, and mean radiance and margin distance were measured. The agreement between margin distance on CLI and histopathology was assessed. Radiation doses to staff were measured. **Results:** Ten of the 12 patients had an elevated tumor radiance on CLI. Mean radiance and tumor-to-background ratio were 560 ± 160 photons/s/cm²/sr and 2.41 ± 0.54 , respectively. All 15 assessable margins were clear on CLI and histopathology. The agreement in margin distance and interrater agreement was good ($\kappa = 0.81$ and 0.912 , respectively). Sentinel lymph nodes were successfully detected in all patients. The radiation dose to staff was low; surgeons received a mean dose of 34 ± 15 μSv per procedure. **Conclusion:** Intraoperative ^{18}F -FDG CLI is a promising, low-risk technique for intraoperative

assessment of tumor margins in BCS. A randomized controlled trial will evaluate the impact of this technique on reexcision rates.

Key Words: Cerenkov luminescence imaging; breast-conserving surgery; tumor margins; ^{18}F -FDG; sentinel lymph node biopsy

J Nucl Med 2017; 58:891–898

DOI: 10.2967/jnumed.116.181032

In early-stage breast cancer, the primary treatment option for most women is breast-conserving surgery (BCS) by wide local excision (WLE) of the tumor. WLE often fails to achieve clear surgical margins, and on average 20% of patients who undergo BCS will require repeated surgery to achieve clear margins (1) (although this may vary because there is no global agreement of the definition of clear margins). Reoperations potentially have several negative consequences including delayed commencement of adjuvant therapy, worse cosmesis, increased patient anxiety, and costs (2,3).

There have been several attempts to assess surgical margins intraoperatively to reduce breast cancer reoperation rates after WLE (1). Techniques evaluated to date include specimen radiography, intraoperative ultrasound, touch imprint cytology, frozen section, and radiofrequency spectroscopy. However, these all have limitations in terms of adequate performance, practicality, or cost-effectiveness (1). Experimental methods evaluated include Raman spectroscopy, ambient mass spectrometry, optical coherence tomography, diffuse reflectance spectroscopy, confocal microscopy, and (targeted) fluorescence imaging (1). Each of these techniques has unique limitations, and the diagnostic performance remains to be evaluated in large-scale studies.

PET using ^{18}F -FDG is a powerful tool for in vivo imaging of breast cancer. Although whole-body PET has limited diagnostic sensitivity for primary breast cancer, high-resolution PET imaging with positron emission mammography has shown high sensitivity (92%–96%) and specificity (84%–91%) for breast cancer diagnosis (4–6). Intraoperative high-resolution imaging of ^{18}F -FDG could

Received Jul. 14, 2016; revision accepted Oct. 26, 2016.

For correspondence or reprints contact: Arnie Purushotham, Department of Research Oncology, 3rd Floor Bermondsey Wing, Guy's Hospital, SE1 9RT, London, U.K.

E-mail: arniepurushotham@gmail.com

Published online Dec. 8, 2016.

COPYRIGHT © 2017 by the Society of Nuclear Medicine and Molecular Imaging.

therefore provide a powerful tool for surgical guidance. However, intraoperative PET is impractical because of the large size and expense of a PET scanner and PET's low spatial resolution. Development of a compact, high-resolution, intraoperative PET scanner could address these limitations.

Recently, it has been discovered that PET imaging agents emit optical photons via a phenomenon called Cerenkov luminescence (7). Cerenkov photons are generated by positrons traveling at super-relativistic speeds in tissue. Optical imaging of Cerenkov photons emitted by PET agents is an emerging imaging modality called Cerenkov luminescence imaging (CLI). CLI combines high diagnostic performance and clinical translatability of PET imaging with high spatial resolution and compactness of optical cameras, thus making it a promising technology for intraoperative margin assessment in breast cancer surgery (8).

In this first-in-human clinical trial, we evaluated the feasibility, safety, and preliminary performance of ^{18}F -FDG CLI using a novel intraoperative CLI camera to assess tumor margin status in breast cancer patients undergoing WLE with sentinel lymph node biopsy (SLNB) or with axillary lymph node dissection (ALND).

MATERIALS AND METHODS

Intraoperative ^{18}F -FDG CLI in BCS

Patient Recruitment and Patient Preparation on Day of Surgery. Research Ethics Committee approval was obtained before patient recruitment (ClinicalTrials.gov identifier NCT02037269). Between June 2014 and February 2016, patients with histologically confirmed invasive breast cancer on core biopsy with or without associated ductal carcinoma in situ (DCIS), due to undergo primary BCS, and SLNB or ALND, were recruited at Guy's Hospital in London after written informed consent was obtained. Exclusion criteria were age younger than 30 y, previous surgery or radiotherapy to the ipsilateral breast in the preceding 2 y, neoadjuvant systemic therapy, pregnancy or lactation, a blood glucose level of 12 mmol/L or more on the day of surgery, and known hypersensitivity to ^{18}F -FDG. Women of childbearing age required a negative pregnancy test (by β -HCG qualitative analysis), history of surgical sterilization, or history of amenorrhea in the past 12 mo.

On the day of surgery, patients scheduled to undergo SLNB received a periareolar intradermal injection of 150 MBq of $^{99\text{m}}\text{Tc}$ -albumin-nanocolloid (Nanocoll; GE Healthcare, U.K.). The increased $^{99\text{m}}\text{Tc}$ activity of 150 MBq was calculated on the basis of the results from 2 lead-in cross-talk studies (supplemental materials [available at <http://jnm.snmjournals.org>]). Patients were then injected intravenously with ^{18}F -FDG (5 MBq/kg; up to a maximum of 300 MBq), and typically 45–60 min after ^{18}F -FDG injection they were taken to the operating theater.

Surgery and Intraoperative Specimen Radiography

After induction of anesthesia, patients due to undergo SLNB received a periareolar subdermal injection of 2 mL of Patent Blue V (Guerbet, France) and 3 mL of normal saline. To minimize radiation exposure to theater staff by reducing the time spent near the patient, a standard breast operating set was prearranged on a sterile tray. Surgery to the breast was performed ahead of SLNB/ALND to minimize signal intensity reduction from radiotracer decay in the time between ^{18}F -FDG injection and CLI. The WLE specimen was excised using monopolar diathermy (Valleylab Force FX electrosurgical generator [Medtronic] with HCP-01 Skintact surgical pencil). The excised specimen was orientated with sutures and metal surgical clips as per local protocol.

Postexcision WLE specimens were x-rayed intraoperatively (Faxitron Bioptics), and excision of cavity shave margins was performed if the tumor was deemed to be close to the edge of the specimen on radiography.

After excision of the WLE specimen, SLNB or ALND was performed. For SLNB, a Europrobe 3 γ -probe with a high-energy collimator was used (Eurorad SA). Sentinel lymph nodes (SLNs) were defined as nodes that were radioactive, blue, or palpable (9). The number of excised SLNs, the *ex vivo* SLN γ -probe signal (counts per second), and the presence of blue nodal discoloration were recorded. On completion of the procedure, the γ -probe background signal in the axilla was measured.

Intraoperative CLI of WLE Specimens and Lymph Nodes

After specimen radiography, CLI of the WLE specimen was performed using an investigational intraoperative CLI system (Light-point Medical Ltd., U.K.). This system consists of a custom-built light-tight dark box containing 2 optical pathways: 1 for CLI and 1 for white-light imaging for anatomic reference (Fig. 1A). The CLI pathway includes a fast $f/95$ lens and a reflex mirror to fold the optical pathway into an electron-multiplying charge-coupled device (EMCCD) camera. The field of view of the CLI camera is 8×8 cm, and the acquisition matrix is 512×512 to give a pixel resolution of $156.25 \mu\text{m}$. The EMCCD is thermoelectrically cooled to -80°C and radiation-shielded with lead to prevent annihilation photons from scintillating in the EMCCD chip—that is, gamma strikes. The white-light imaging pathway provides a photographic reference image using a standard complementary metal oxide semiconductor camera.

The WLE specimen was positioned on a specimen table (Fig. 1B), the margin of interest was placed in the center of the field of view using the surgical sutures to guide orientation, and the specimen was subsequently imaged.

After intact WLE specimen imaging, the surface of the specimen was immediately inked intraoperatively to preserve its orientation for histopathologic analysis (Supplemental Fig. 1A). Six distinct ink colors (Davidson; Bradley Products Inc., USA) were applied to the 6 margins. The inked specimen was then incised through the posterior margin to visualize the primary tumor and tumor margins, and the incised WLE specimen was imaged (Supplemental Figs. 1B and 1C). In 1 patient, sequential images over a 50-min time period were acquired to determine the half-life of the radiance observed in the tumor.

The first 10 patients were included in the optimization dataset and the remaining 12 patients in the analysis dataset. In the first 10 patients, the image acquisition protocol was optimized by testing different image acquisition times (100, 300, 400 s) and pixel binning settings (2×2 , 4×4 , 8×8). A 300-s acquisition time and 8×8 pixel binning was found to provide sufficient sensitivity for tumor detection and acceptable spatial resolution (1.25 mm) within a time window feasible for intraoperative use, and these settings were used in the remaining 12 patients included in the analysis dataset. On completion of WLE CLI, the activity of the WLE specimen was estimated using a scintillation monitor (type 41/44A; ThermoScientific, USA) or handheld radiation spectrometer (Raymon10 GR1; Kromek PLC). SLNs were also imaged intraoperatively with CLI using the same imaging settings.

After imaging was completed, WLE specimens were sent for histopathologic analysis as per standard practice.

Radiation Safety Monitoring

Radiation safety monitoring was performed to ensure that safe working practices were maintained and that work was compliant with U.K. legislation regarding ionizing radiation (10–12). Before commencing the study, all staff received training to become familiar with radiation control procedures and occupational risks and learned how to minimize exposure without compromising patient care. Staff members were issued electronic personal radiation dose monitors (PDM-112 and PDM-122; Hitachi-Aloka Medical Ltd.) for the body and thermoluminescent ring dosimeters for extremities (Landauer).

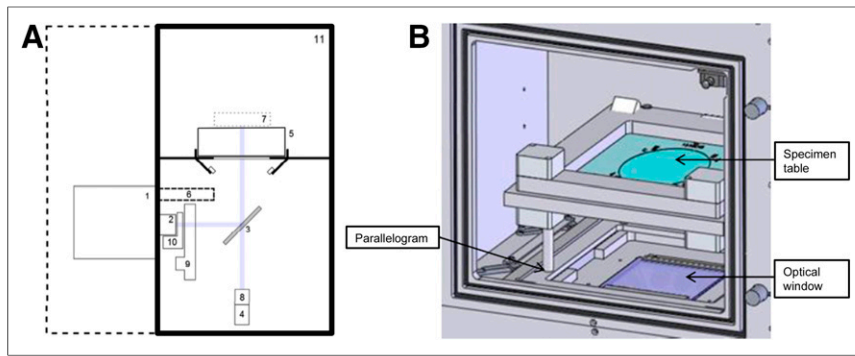


FIGURE 1. Investigational intraoperative CLI specimen camera. (A) Schematic diagram. Component labels: (1) EMCCD camera, (2) f/.95 lens, (3) Hinged reflex mirror, (4) complementary metal oxide semiconductor reference camera, (5) specimen table, (6) lead radiation shielding for EMCCD camera, (7) focal zone, (8) fixed lens for reference camera, (9) filter wheel, (10) LED RGB light array, (11) Specimen chamber. Purple line shows optical paths for EMCCD camera and reference camera as determined by angle of reflex mirror. (B) Specimen chamber. Specimen table is placed on a parallelogram to facilitate accurate positioning of specimen in center of image.

Radiation contamination monitoring of staff, rooms, equipment, and waste was performed after each procedure using a scintillation monitor (type 41/44A, Series 300 mini-monitor; ThermoScientific). Because ^{99m}Tc has a longer half-life (6.02 h) than ¹⁸F (110 min), the radioactive

waste storage requirements for CLI procedures are similar to standard SLNB procedures. The time taken for the various stages of the procedure, that is, from induction of anesthesia to recovery, were recorded.

Histopathology

Histopathologic analysis was performed as per U.K. national guidelines: the WLE specimen was sliced at 2-mm intervals, and representative sections of the tumor and all 6 relevant margins were selected by the pathologist, processed, and embedded in paraffin wax, and 3- to 4- μ m sections were cut and stained with hematoxylin and eosin. Microscopic margin distance measurements were performed by a consultant breast pathologist. Microscopic invasive tumor size and whole-tumor size (including DCIS extending from the main invasive mass) were also measured. Positive margins were defined as invasive cancer or DCIS less than 1 mm from the specimen surface. The histologic margin distances were reported in increments of 1 mm, but margins more than 5 mm were reported as greater than 5 mm. The pathologist was blinded to the interpretation of the Cerenkov luminescence images.

TABLE 1
CLI and Postoperative Histopathology Results for Each Patient in Analysis Dataset

Patient	Tumor type	Histologic grade invasive (1-3)	ER/HER2 status of invasive cancer (Pos/neg)	Mean tumor radiance (photons/s/cm2/sr)	TBR	Margin distance CLI surgeons 1 and 2* (mm)	Margin distance histopathology (mm)	Tumor size CLI surgeons 1 and 2* (mm)	Invasive tumor size histopathology† (mm)	Whole tumor size histopathology† (mm)
1	NST DCIS	2	Pos/Neg	—‡	—	—	—	—	13	13
2	NST DCIS	3	Neg/Pos	453.59	2.34	6, 6	>5	*¶	22	22
3	NST	3	Neg/Neg	871.16	3.22	2, 2	3	20, 18	20	20
						28, 30	>5			
4	NST DCIS	3	Neg/Neg	—‡	—	—	—	—	14	14
5	NST DCIS	3	Pos/Neg	405.76	2.03	2, 3	5	18, 18	20	20
6	ILC	2	Pos/Neg	544.04	2.44	9, 9	>5	20, 19	22	22
7	NST	3	Pos/Neg	667.47	2.72	10, 11	>5	*¶	25	25
8	NST DCIS	2	Pos/Neg	308.30	1.63	6, 8	>5	19, 19	15	35
						16, 15	>5			
9	NST DCIS	3	Pos/Neg	593.93	3.08	14, 13	>5	14, 15	18	19
						6, 7	>5			
10	NST DCIS	3	Pos/Neg	648.29	2.46	8, 8	>5	22, 22	19	29
11	NST DCIS	2	Pos/Neg	466.03	2.54	15, 14	>5	13, 11	13	13
12	NST DCIS	3	Pos/Neg	637.08	1.63	9, 9	>5	12, 10	14	14
						30, 31	>5			
						22, 22	>5			

*Margin distance and tumor size are shown for surgeons 1 and 2, respectively.

†Histopathologic tumor size displayed in table is tumor size measured in same direction as tumor size measurement on CLI. In patients 3, 11, and 12, largest invasive and whole tumor size (i.e., extent of DCIS and invasive cancer) were measured in different direction, and were 32, 33, and 25 mm, respectively.

‡No elevated tumor radiance on CLI.

¶Presence of orientation inks prevented measuring tumor size on CLI.

ER = estrogen receptor; HER2 = human epidermal growth factor receptor 2; NST = invasive carcinoma of ductal/no special type; Pos = positive; Neg = negative; ILC = invasive lobular carcinoma.

Image Analysis

All Cerenkov luminescence and radiography images were analyzed postoperatively to provide a controlled and standardized analysis environment. Measurements of the mean radiance (photons/s/cm²/sr) were performed by drawing regions of interest on the unprocessed Cerenkov luminescence images. Regions of interest were selected in areas showing increased signal intensity (tumor) and no increased signal (tissue background). Tumor-to-background ratios (TBRs) were calculated. γ -strikes were excluded from region-of-interest analysis. The tumor radiance from the sequential incised WLE images was fit to a monoexponential, to determine the radiance half-life.

Assessment of margin status on CLI was performed on the incised WLE specimen images. The analysis was done independently by 2 experienced breast surgeons and performed before analysis of the radiography images to prevent potential confirmation bias from a priori knowledge of the radiologic margin status. Before analysis Cerenkov luminescence images were processed by applying a median filter (filter size range, 5–10; filter threshold range, 10–15) and gaussian filter (filter width, 1; filter threshold, 0.5). A stronger gaussian filter (filter width, 4 or 5) was applied to images with a low TBR to increase the visibility of the tumor. The preoperative diagnostic information that would typically be

available to the surgeon was provided including patient age; clinical, mammographic, and ultrasound tumor size; screen detected (Y/N); and histologic tumor type, grade, and receptor status on core biopsy. Per patient, a color image containing information on specimen orientation was shown together with a gray-scale image and Cerenkov image. All images were displayed on a standard computer monitor (23", 1,920 × 1,080 pixels, 250 cd/m² luminance). The gray-scale image was overlaid with the Cerenkov signal to provide a fused image containing both functional and anatomic information. The leveling was set using the software's default leveling and manually adjusted based on the surgeon's clinical judgment. Both surgeons then independently reported whether an elevated radiance from the tumor could be identified on CLI; in patients displaying an elevated tumor radiance the margin distance of the margins visible in the image was measured using the ruler function in the imaging software (Mirada XD3; Mirada Medical). The total time required to complete margin assessment was approximately 2 min per patient. As an exploratory outcome measure, tumor size was also measured. On completion of the measurements, surgeons were asked whether, given the Cerenkov luminescence image, they would have performed a cavity shaving had the image been available at the time of surgery. Surgeons also scored image quality on a 5-point Likert scale: 1, very poor—image not interpretable; 2, poor but interpretable; 3, fair; 4, good; 5, very good.

After Cerenkov luminescence image analysis, specimen radiography image analysis was performed on a Coronis 3MP screen (20.8", 1,536 × 2,048 pixels, 500 cd/m² luminance) using standard PACS imaging software (GE Healthcare). Surgeons were presented with the same preoperative diagnostic information, but the images were shown in a different order to avoid potential sequential bias. The number of surgical marker clips was noted, and the reliability of specimen orientation assessed. If the orientation was considered reliable, the margin distance and tumor size on radiography was measured. Whether an additional cavity shaving would have been performed based on the radiography image was also noted.

The final histopathology results of the surgically excised tissue were not available at the time of Cerenkov luminescence image and radiography image analysis and could therefore not bias the surgeon's assessment.

Statistics

Weighted κ coefficients (κ) were calculated to assess the agreement in margin distance between CLI and definitive histopathology and to assess the interrater agreement between surgeons (irr package, version 3.2.2, R statistical software). A κ greater than 0.75 was considered good agreement (13). Agreement between histologic tumor size and tumor size on CLI and radiography, respectively, was assessed by calculating the mean difference in tumor size \pm SD and intraclass correlation coefficients (ICCs) (SPSS, version 23.0; IBM).

RESULTS

Intraoperative Imaging of WLE Specimens

A total of 22 patients were included in the study. The CLI results and postoperative

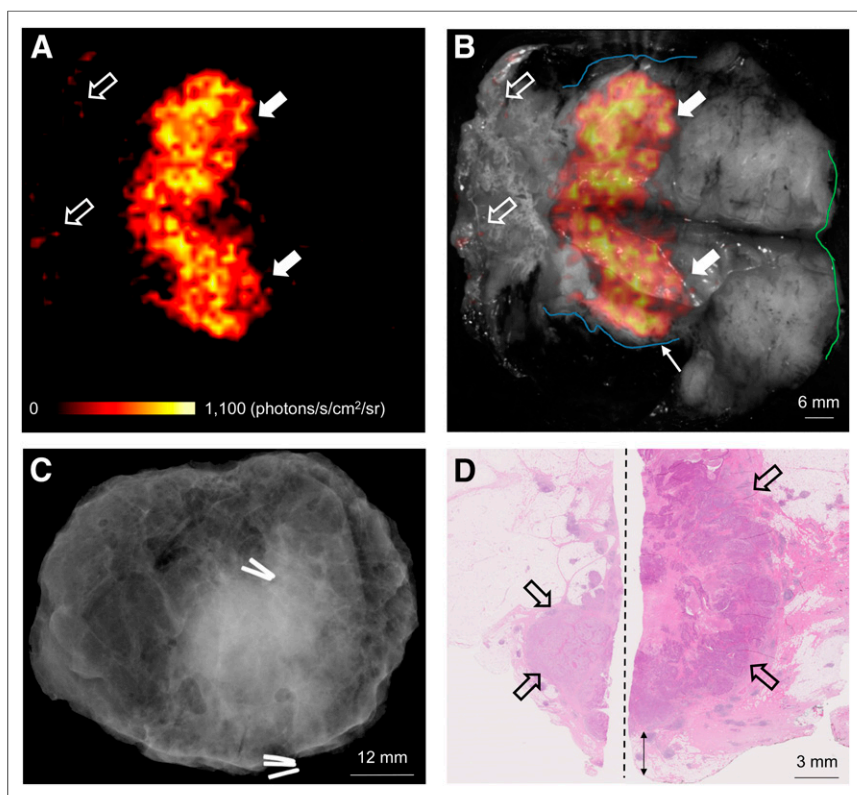


FIGURE 2. WLE specimen from patient with grade 3, estrogen receptor–negative/human epidermal growth factor receptor 2–negative, NST carcinoma. (A) Cerenkov image. (B) Gray-scale photographic image overlaid with Cerenkov signal. Increased signal from tumor is visible (white arrows); mean radiance is 871 ± 131 photons/s/cm²/sr, mean TBR is 3.22. Both surgeons measured posterior margin (outlined in blue) as 2 mm (small arrow); cavity shaving would have been performed if image had been available intraoperatively. Medial margin (outlined in green) measured > 5 mm by both surgeons. Pathology ink prevented assessment of lateral margin; phosphorescent signal is visible (open arrows). (C) Specimen radiography image. Absence of 1 surgical clip to mark anterior margin and odd position of the superior margin clip prevented reliable margin assessment. (D) Combined histopathology image from 2 adjacent pathology slides on which posterior margin (bottom of image) and part of primary tumor are visible (open arrows). Distance from posterior margin measured 3 mm microscopically (double arrow). Medial margin is >5 mm (not present in image).

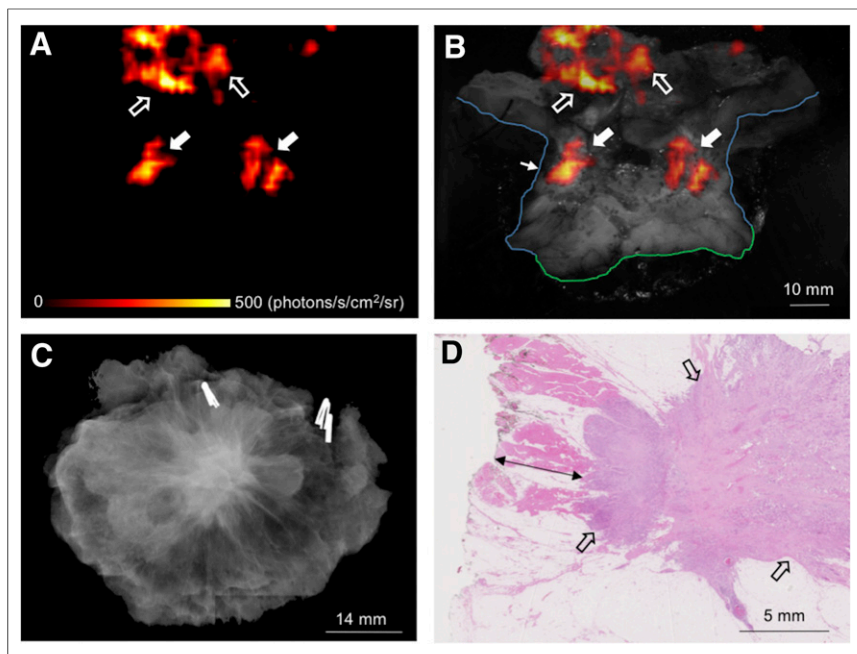


FIGURE 3. WLE specimen from patient with grade 3, estrogen receptor-positive/human epidermal growth factor receptor 2-negative, NST carcinoma admixed with high-grade DCIS. (A) Cerenkov image. (B) Gray-scale photographic image overlaid with Cerenkov signal. Increased signal from tumor is visible (white arrows); mean radiance is 406 ± 51 photons/s/cm²/sr, mean TBR is 2.03. A phosphorescent signal from orange pathology ink is visible (open arrows). Posterior margin (outlined in blue) is 2 or 3 mm on CLI as measured by surgeons 1 and surgeon 2, respectively (small arrow). Both surgeons would have performed cavity shaving. Medial margin (outlined in green) is > 5 mm. (C) Specimen radiography image. All 4 radial margins were > 5 mm, and both surgeons indicated they would not have performed cavity shaving. (D) Histopathology image showing posterior margin (left side of image) and part of tumor (open arrows). Posterior margin was 5 mm distant histologically (double arrow).

histopathology results from the 12 patients included in the analysis dataset are shown in Table 1. The mean administered ¹⁸F-FDG activity was 295 ± 18 MBq (range, 259–325 MBq). The mean time between ¹⁸F-FDG injection and WLE excision was 86 ± 26 min (range, 50–146 min), and the mean time between ¹⁸F-FDG injection and commencement of Cerenkov luminescence image acquisition was 118 ± 26 min (range, 88–180 min).

Tumor margin assessment was performed on incised WLE specimen images to allow for visualization of the tumor extent and to avoid image artifacts created by the monopolar diathermy. Ten of the 12 patients in the analysis dataset had elevated tumor radiance on CLI (Table 1). The mean tumor radiance and TBR in these 10 patients was 560 ± 160 photons/s/cm²/sr (range, 308–871 photons/s/cm²/sr) and 2.41 ± 0.54 (range, 1.63–3.22), respectively. The half-life of the tumor radiance was 115.5 min, which is consistent with the 109.8-min half-life of ¹⁸F. This concordance supports that the detected tumor radiance is Cerenkov luminescence from ¹⁸F-FDG. The mean radioactivity in the WLE specimen at the time of CLI was 90 ± 48 kBq in patients with an elevated radiance, and in the 2 patients without an elevated radiance radioactivity it was 14 and 19 kBq, respectively.

In the 10 patients with elevated tumor radiance, a total of 60 margins could be assessed histologically, 26 margins were evaluable on specimen radiography, and 15 margins were assessable on CLI. Of the 45 histologic margins that were not evaluable on CLI, 40 were not in the field of view of the Cerenkov luminescence image, and 5 could not be assessed because of migration of the specimen orientation ink onto the margin edge, preventing optical margin

interrogation. Eighteen of the 60 histologic margins were not assessable on specimen radiography because of the inability to reliably orientate the specimen on the radiography image, and 16 margins were not in the image field of view.

The margin distance from the 15 margins as measured on CLI and histopathology is shown in Table 1. Two margins measured between 1 and 5 mm on CLI and histopathology (Figs. 2 and 3); the remaining 13 margins were greater than 5 mm by both modalities. There was good agreement between the histologic margin distance and the margin distance on CLI as measured by both surgeon 1 and surgeon 2, respectively (κ surgeon 1, 0.76; κ surgeon 2, 0.86). The agreement in margin distance between surgeons was also good ($\kappa = 0.91$).

Five margins could be assessed on both CLI and specimen radiography, and all were greater than 5 mm on both modalities, as well as histologically. An example of a CLI, radiography, and histopathology image from a patient with greater than 5-mm resection margin widths is shown in Figure 4.

Two patients (17%) had a positive margin on postoperative histopathologic analysis; both were medial margins with DCIS less than 1 mm distant. These margins were not visible in the Cerenkov luminescence image because specimen incision had exposed only the superior, inferior, and posterior margins; the medial margin could therefore not be assessed.

In 8 of the 10 patients, tumor size could be measured on CLI and compared with histopathology: the agreement is shown in Table 1. In 2 patients, the orientation inks prevented measurement of tumor size on CLI. Invasive tumor size showed excellent agreement; mean difference for both surgeons combined was -0.84 ± 2.8 mm. ICC was 0.84 and 0.81 for surgeons 1 and 2, respectively. Whole-tumor size was underestimated on CLI; the mean difference for both surgeons combined was -4.7 ± 5.0 mm. ICC was 0.65 and 0.69 for surgeons 1 and 2, respectively. Interrater agreement between surgeons was excellent (ICC = 0.97).

The agreement between invasive tumor size on histopathology and on radiography was good; the mean difference for both surgeons combined was 1.0 ± 3.1 mm. ICC was 0.56 and 0.58 for surgeons 1 and 2, respectively. Whole-tumor size was underestimated on radiography; the mean difference for both surgeons combined was -5.2 ± 8.9 mm.

Cerenkov luminescence image quality in the 10 patients with successful CLI was scored as 4.3 (range, 4–5) by both surgeons.

Cerenkov luminescence image quality in the 10 patients with successful CLI was scored as 4.3 (range, 4–5) by both surgeons.

SLN Detection and ¹⁸F-FDG Cerenkov Lymph Node Imaging

SLNB was performed in 21 of the 22 patients; 1 patient underwent an ALND. SLNs were successfully identified in all 21 patients. A total of 43 SLNs were removed. The average number of SLNs per patient was 2 (range, 1–4). Two of the 21 SLNB patients had macrometastatic SLNs.

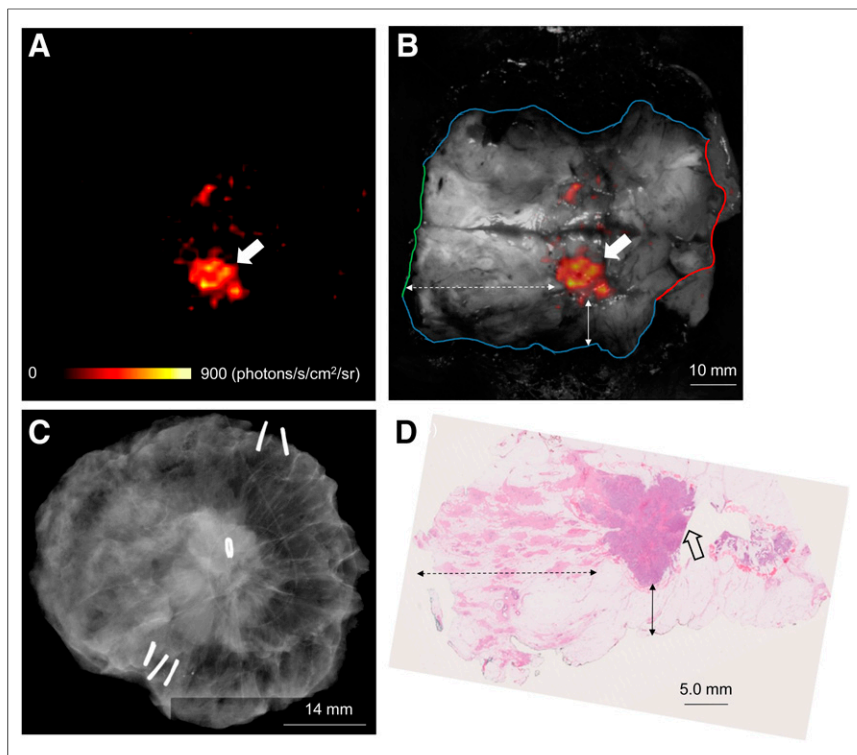


FIGURE 4. WLE specimen from patient with grade 3, estrogen receptor-positive/human epidermal growth factor receptor 2-negative, NST carcinoma admixed with high-grade DCIS. (A) Cerenkov image. (B) Gray-scale photographic image overlaid with Cerenkov signal. Elevated signal (white arrow) from tumor can be seen. Mean radiance is 637 ± 47 photons/s/cm²/sr; mean TBR is 1.63. Both surgeons measured posterior margin (outlined in blue), medial margin (outlined in green), and lateral margin (outlined in red) distances as > 5 mm; cavity shaving would not have been performed on basis of Cerenkov luminescence image. (C) Specimen radiography image. All 4 radial margins were > 5 mm as measured by both surgeons and did not prompt resection of cavity-shave margins. (D) Histopathology image from large-format pathology block. Tumor is > 5 mm from posterior margin (solid arrow), medial margin (dashed arrow), and lateral margin (not visible in image).

The mean γ -probe signal of the hottest SLN per patient was $4,991 \pm 2,521$ counts per second (range, 170–8,500). The mean γ -probe signal of the second hottest SLN was $2,505 \pm 2,632$ counts per second (range, 50–7,368). Mean axillary background signal, measured in 13 patients, was 192 ± 70 counts per second (range, 55–270). This signal is lower than the ¹⁸F-FDG γ -probe cross-talk measured in the lead-in study (supplemental materials) and is mainly due to the longer time between ¹⁸F-FDG injection and SLNB (mean, 93 ± 34 min). A total of 7 nodes had a γ -probe signal below the background signal; 6 of these were blue. This indicates the importance of using the combined technique of radioisotope and blue dye in ¹⁸F-FDG CLI-guided breast surgery, because low-uptake nodes may be missed if γ -probe detection is used alone.

All SLNB procedures were performed with the monopolar diathermy device, and due to the observed image artifact from diathermy on CLI the SLN images were uninterpretable.

Radiation Dose to Staff

A summary of the whole-body effective radiation dose to primary personnel from all 22 procedures is shown in Table 2. Surgeons received the highest mean and maximum dose of 34 and 74 μ Sv, respectively. The mean duration of surgery was 39 ± 11 min (range,

21–61 min) during which the surgeon was generally less than 0.5 m from the patient. The mean radiation dose to the left and right hand of the surgeon was 126 ± 95 μ Sv (range, 0–250 μ Sv) and 78 ± 75 μ Sv (range, 0–200 μ Sv), respectively. The mean and maximum radiation dose received by the anesthetist standing at approximately 1 m from the patient, with closer patient contact at the time of induction of anesthesia and at the end of the procedure, was 11 and 18 μ Sv, respectively. Surgical equipment had low levels of radioactive contamination, which was undetectable 1–3 d later. No staff members were found to be contaminated with radioactivity after the procedures.

DISCUSSION

This first-in-human study evaluated the feasibility of intraoperative ¹⁸F-FDG CLI for assessing tumor margin status in patients with invasive breast cancer undergoing BCS and SLNB or ALND. Tumor margin assessment on CLI could be performed in 10 of the 12 patients in the analysis dataset, and there was strong agreement between CLI and definitive histopathology on margin width. An exploratory outcome measure assessed the correlation between tumor size on CLI and histopathology; the size on CLI and histopathology correlated well for invasive cancer, whereas whole-tumor size (invasive with associated DCIS) was underestimated on CLI. Results from the radiation monitoring program demon-

strated that the procedure can be performed safely while maintaining low radiation exposures to the staff involved.

In 2 patients, margin assessment could not be performed because the tumors did not display elevated radiance on CLI. The absence of signal in these patients is probably due to the small tumor size, a factor known to be associated with lower ¹⁸F-FDG uptake (14), and the late time points at which these tumors were imaged (135 and 180 min after ¹⁸F-FDG injection; the first and third longest injection-imaging time of all patients). Unsuccessful CLI because of the absence of a detectable tumor signal highlights the importance of ongoing developments focused on improving detection sensitivity of camera systems to aid detection of tumors with low ¹⁸F-FDG uptake including lower grade tumors and DCIS (4).

Since its discovery in 2009, CLI has rapidly emerged as a powerful technique for cancer imaging. CLI is readily translatable to the clinic because of existing regulatory approval and widespread availability of PET imaging agents (15). In contrast, targeted fluorescence imaging requires prohibitive clinical development times and capital investment for regulatory and reimbursement approval of novel imaging drugs (16). Three clinical pilot studies of CLI have been published to date. These have focused on the use of CLI to image radiopharmaceutical uptake in the thyroid, CLI for noninvasive detection of nodal disease, and

TABLE 2
Measured Effective Radiation Doses by Occupation from 22 Surgical Procedures

Staff group	<i>n</i>	Mean effective dose per procedure ± SD (μSv)	Range (μSv)	Estimated no. of procedures per individual per year* (ICRP [20-mSv annual limit])	Estimated no. of procedures per individual per year* (USNRC [50-mSv annual limit])
Surgeon	46	34 ± 15	8–74	270	676
Anesthetist	22	11 ± 5	0–18	1,111	2,778
Nuclear medicine technologist	22	9 ± 4	1–15	1,333	3,333
Anesthetist assistant	22	6 ± 3	0–11	1,818	4,545
Trial cocordinator	21	5 ± 2	1–10	2,000	5,000
Recovery nurse	43	4 ± 3	0–14	1,429	3,571
Scrub nurse	22	2 ± 1	0–5	4,000	10,000
Periphery nurse	23	1 ± 1	0–4	5,000	12,500
Research fellow	36	1 ± 2	0–13	1,538	3,846
Ward nurse	15	0	0–1	20,000	50,000
Tissue biobank practitioner	14	0	0–1	20,000	50,000

*Based on maximum effective dose per procedure per staff group.

ICRP = International Commission on Radiological Protection; USNRC = U.S. Nuclear Regulatory Commission.

Cerenkov luminescence endoscopy to aid detection of cancerous lesions in the gastrointestinal tract (17–19). To our knowledge, this is the first report of intraoperative CLI. Its high-resolution, small-size imaging equipment and minute-scale image acquisition (5 min) and image analysis (~2 min) times make CLI of particular interest for image-guided surgery. The feasibility of intraoperative CLI as shown in this study in combination with the wide applicability of ¹⁸F-FDG across a range of solid cancers provides a stepping stone for clinical evaluation of this technology in other cancer types.

The low radiation exposure to staff found in this study is in accordance with previously reported exposure levels from ¹⁸F-FDG-guided breast surgery procedures (20,21) and comparable to the radiation dose reported for interventional cardiology procedures (1–50 μSv) (22). The number of ¹⁸F-FDG CLI-guided BCS procedures that could be performed in a routine clinical setting depends on the occupational limits on radiation exposure per country (Table 2). In the United Kingdom and United States, the occupational annual dose limit is 20 (23) and 50 mSv (24), respectively. Good practice would dictate that the radiation exposure from a procedure should be kept As Low As Reasonably Achievable, that is, well below the dose limits. In practice in the United Kingdom, if workers are likely to receive annually more than 6 mSv they would be designated a classified worker, necessitating annual medical surveillance and longer term record keeping of their radiation exposure.

Image artifacts on CLI from tissue excised with the monopolar diathermy device prevented tumor margin assessment on intact WLE specimens and assessment of SLNs. Although the source of this false signal is not yet fully understood, current evidence from preclinical experiments points toward long-lived, thermally induced chemiluminescence (25). Because the emission seems to be related to temperature, which can reach up to 250°C at the tip of the diathermy device, electrosurgical devices that operate at much lower temperatures are currently being tested (26). In addition to potentially facilitating margin assessment on intact

WLE specimens, an advantage of low-temperature devices over monopolar diathermy is the reduced collateral tissue damage, which could also improve the accuracy of assessing tumor resection margins on histopathology (27).

Although CLI of incised WLE specimens is feasible for assessing tumor margin status, this approach has some limitations over margin assessment on intact specimens. First, migration of the wet pathology ink onto the margin edge immediately after specimen incision hinders margin interpretation with CLI. Methods to accelerate drying of inks by applying acetic acid to the painted tissue or using fast-drying inks may be solutions to this problem, but this has not been tested in this study. Second, in our institution specimen incision could be performed only through the posterior margin to ensure accurate postoperative histologic assessment of radial margins. Consequently, only a limited number of margins could be assessed with CLI per patient, and 2 histologically positive margins that were not visible in the Cerenkov luminescence image were therefore missed. To assess more margins per patient specimen incision may be performed in multiple planes, but good communication between surgeons and pathologists is paramount to not compromise patient care.

A randomized, controlled, multicenter clinical study is scheduled to commence in early 2017, with the first patient expected to be recruited in February 2017, to evaluate the effect of intraoperative ¹⁸F-FDG CLI on reoperation rate and quality of life in BCS (ClinicalTrials.gov identifier NCT02666079). The study will run across an anticipated 8 study sites in the United Kingdom and Germany and use the CE-marked (CE is Conformité Européenne [or European Conformity]) LightPath Imaging System (Lightpoint Medical Ltd., U.K.). The smaller field of view of 6 × 6 cm and improved imaging software may provide substantial improvements in sensitivity over the investigational CLI camera used in the present study. By analyzing larger subgroups of patients with a range of tumor types (including DCIS), size, histologic grades, and hormone receptor status, further insight should be obtained into which breast cancer patient populations may most benefit from CLI-guided surgery.

CONCLUSION

Intraoperative ^{18}F -FDG CLI in BCS for invasive breast carcinoma is a promising and low-risk procedure. CLI of incised WLE specimens provides high-resolution functional information that allows surgeons to accurately assess margin status with good correlation to gold-standard histopathologic examination. Further work, focused on suppressing the optical signal from the monopolar diathermy device, will assist margin assessment on intact WLE specimens and potentially identification of SLN metastases on CLI. SLNB can be performed successfully during ^{18}F -FDG CLI-guided surgery using 150 MBq of $^{99\text{m}}\text{Tc}$ -nanocolloid and blue dye. On the basis of the results of this study, a larger randomized controlled study is warranted to evaluate the impact of intraoperative ^{18}F -FDG on reoperation rate and quality of life in BCS.

DISCLOSURE

This study was supported by funding from Innovate U.K., Cancer Research U.K. King's Health Partners Experimental Cancer Medicine Centre, Guy's and St Thomas' Charity, and the National Institute for Health Research (NIHR) Biomedical Research Centre at Guy's and St Thomas' NHS Foundation Trust and King's College London. David S. Tuch is an employee of and a shareholder in Lightpoint Medical Ltd. The views expressed are those of the authors and not necessarily those of the NHS, the NIHR or the Department of Health. No other potential conflict of interest relevant to this article was reported.

ACKNOWLEDGMENTS

We gratefully acknowledge the excellent support from the King's Health Partners Cancer Biobank, Breast Cancer NOW, Viapath pathology services, and the King's College London and Guy's and St Thomas' PET Centre.

REFERENCES

1. St John ER, Al-Khudairi R, Ashrafian H, et al. Diagnostic accuracy of intraoperative techniques for margin assessment in breast cancer surgery: a meta-analysis. *Ann Surg*. 2017;265:300–310.
2. Munshi A, Kakkar S, Bhutani R, Jalali R, Budrukkar A, Dinshaw KA. Factors influencing cosmetic outcome in breast conservation. *Clin Oncol (R Coll Radiol)*. 2009;21:285–293.
3. Abe SE, Hill JS, Han Y, et al. Margin re-excision and local recurrence in invasive breast cancer: a cost analysis using a decision tree model. *J Surg Oncol*. 2015;112:443–448.
4. Kalinyak JE, Berg WA, Schilling K, Madsen KS, Narayanan D, Tartar M. Breast cancer detection using high-resolution breast PET compared to whole-body PET or PET/CT. *Eur J Nucl Med Mol Imaging*. 2014;41:260–275.
5. Narayanan D, Madsen KS, Kalinyak JE, Berg WA. Interpretation of positron emission mammography and MRI by experienced breast imaging radiologists: performance and observer reproducibility. *AJR*. 2011;196:971–981.
6. Schilling K, Narayanan D, Kalinyak JE, et al. Positron emission mammography in breast cancer presurgical planning: comparisons with magnetic resonance imaging. *Eur J Nucl Med Mol Imaging*. 2011;38:23–36.
7. Das S, Thorek DL, Grimm J. Cerenkov imaging. *Adv Cancer Res*. 2014;124:213–234.
8. Grootendorst MR, Cariati M, Kothari A, Tuch DS, Purushotham A. Cerenkov luminescence imaging (CLI) for image-guided cancer surgery. *Clin Transl Imaging*. 2016;4:353–366.
9. Mansel RE, MacNeill F, Horgan K, et al. Results of a national training programme in sentinel lymph node biopsy for breast cancer. *Br J Surg*. 2013;100:654–661.
10. Health and Safety Executive. The ionising radiations regulations 1999. No. 3232: health and safety executive. Legislation.gov.uk website. <http://www.legislation.gov.uk/uksi/1999/3232/contents/made>. Accessed April 11, 2017.
11. Department of Health. Ionising radiation (medical exposure) regulations 2000 (IRMER). Gov.UK website. <https://www.gov.uk/government/publications/the-ionising-radiation-medical-exposure-regulations-2000>. Accessed April 11, 2017.
12. Department for Environmental, Food and Rural Affairs. The environmental permitting (England and Wales) regulations 2010. Gov.UK website. <https://www.gov.uk/government/publications/environmental-permitting-guidance-core-guidance-2>. Published March 2013. Accessed April 11, 2017.
13. Khan KS, Chien PF. Evaluation of a clinical test. I: assessment of reliability. *BJOG*. 2001;108:562–567.
14. Kumar R, Chauhan A, Zhuang H, Chandra P, Schnall M, Alavi A. Clinicopathologic factors associated with false negative FDG-PET in primary breast cancer. *Breast Cancer Res Treat*. 2006;98:267–274.
15. Spinelli AE, Boschi F. Novel biomedical applications of Cerenkov radiation and radioluminescence imaging. *Phys Med*. 2015;31:120–129.
16. Agdeppa ED, Spilker ME. A review of imaging agent development. *AAPS J*. 2009;11:286–299.
17. Spinelli AE, Ferdeghini M, Cavedon C, et al. First human Cerenkography. *J Biomed Opt*. 2013;18:020502-1–020502-2.
18. Thorek DL, Riedl CC, Grimm J. Clinical Cerenkov luminescence imaging of ^{18}F -FDG. *J Nucl Med*. 2014;55:95–98.
19. Hu H, Cao X, Kang F, et al. Feasibility study of novel endoscopic Cerenkov luminescence imaging system in detecting and quantifying gastrointestinal disease: first human results. *Eur Radiol*. 2015;25:1814–1822.
20. Heckathorne E, Dimock C, Dahlbom M. Radiation dose to surgical staff from positron-emitter-based localization and radiosurgery of tumors. *Health Phys*. 2008;95:220–226.
21. Andersen PA, Chakera AH, Klausen TL, et al. Radiation exposure to surgical staff during F-18-FDG-guided cancer surgery. *Eur J Nucl Med Mol Imaging*. 2008;35:624–629.
22. Durán A, Hian SK, Miller DL, Le Heron J, Padovani R, Vano E. Recommendations for occupational radiation protection in interventional cardiology. *Catheter Cardiovasc Interv*. 2013;82:29–42.
23. International Commission on Radiological Protection (ICRP). The 2007 recommendations of the International Commission on Radiological Protection. ICRP publication 103. *Ann ICRP*. 2007;37:1–332.
24. United States Nuclear Regulatory Commission (USNRC). Standards for protection against radiation. 10 CFR 20.1201. USNRC website. <https://www.nrc.gov/reading-rm/doc-collections/cfr/part020/part020-1201.html>. Accessed January 13, 2017.
25. Sun JS, Tsuang YH, Chen IJ, Huang WC, Hang YS, Lu FJ. An ultra-weak chemiluminescence study on oxidative stress in rabbits following acute thermal injury. *Burns*. 1998;24:225–231.
26. Loh SA, Carlson GA, Chang EI, Huang E, Palanker D, Gurtner GC. Comparative healing of surgical incisions created by the PEAK PlasmaBlade, conventional electrosurgery, and a scalpel. *Plast Reconstr Surg*. 2009;124:1849–1859.
27. Ruidiaz ME, Cortes-Mateos MJ, Sandoval S, et al. Quantitative comparison of surgical margin histology following excision with traditional electrosurgery and a low-thermal-injury dissection device. *J Surg Oncol*. 2011;104:746–754.